Muon spin relaxation as a probe of electron motion in conducting polymers

2004 J. Phys.: Condens. Matter 16 S4779

(http://iopscience.iop.org/0953-8984/16/40/019)

INSTITUTE OF PHYSICS PUBLISHING JOURNAL OF PHYSICS: CONDENSED MATTER

J. Phys.: Condens. Matter **16** (2004) S4779–S4796 PII: S0953-8984(04)85488-2

Muon spin relaxation as a probe of electron motion in conducting polymers

F L Pratt

ISIS Facility, Rutherford Appleton Laboratory, Chilton, Didcot OX11 0QX, UK

Received 29 March 2004
Published 24 September 2004
Online at stacks.iop.org/JPhysCM/16/S4779
doi:10.1088/0953-8984/16/40/019

Abstract

The use of implanted muons to probe the dynamics of electronic excitations in conducting polymers is reviewed. Early work on polyacetylene showed evidence for mobile solitons performing one-dimensional diffusion in the *trans* isomer and localized spins in the *cis* isomer. Subsequent muon studies on a range of conducting polymers have shown evidence for mobile polaronic excitations and microscopic transport properties for these polarons have been derived from the measurements. A theoretical framework was developed by Risch and Kehr to describe the intermittent hyperfine coupling between a static muon and an electron diffusing randomly through a chain of sites. This theory predicts a specific form for both the muon spin relaxation function and the field dependence of the relaxation rate. The experimental data are found to be described well by this model. Intrachain diffusion rates can be extracted from the data; in several cases an interchain diffusion rate can also be measured. The anisotropy of diffusion rates can be as high as 10^4 at low temperatures, reducing typically to 10^2 or less at room temperature. The importance of molecular vibrational modes in controlling the electronic motion in the polymer has been shown.

The topic of conducting polymers has developed steadily from a field of novel physics and chemistry into an important area of technology, involving the production of commercial electronic and optoelectronic devices [1, 2]. The nature of the charge carriers and the mechanisms of charge motion in such polymeric materials are fundamental to their operation. Various types of measurement can be applied to determine carrier transport properties; one class of techniques are spin dynamical probes, which focus on electronic excitations with spin and measure the fluctuating magnetic field at a probe position due to the motion of this spin. Spin dynamical techniques in the form of ESR and NMR investigations have been used extensively to study carrier diffusion in anisotropic conductors and many studies on doped conducting polymers have been reported (for a review of the application of spin

dynamical techniques using magnetic resonance to conducting polymers, see [3]). Alongside the conventional magnetic resonance techniques, μSR has also emerged as an alternative spin dynamical probe which can be applied to such systems. In contrast to ESR and NMR, μSR has the unique feature that, in many situations, it can both generate an excitation by chemical reaction with the system and also act as a sensitive probe of the dynamics of this excitation. This is particularly the case in conjugated polymer systems, where muonium forms readily and rapidly reacts with the unsaturated bonds. A particular interest in these polymeric systems is that, due to strong electron–lattice coupling, the mobile electronic excitations take the form of solitons and polarons—properties of these excitations forming the basis for a range of molecular electronic devices. μSR spin dynamics is a particularly powerful probe for conductors with very low concentrations of carriers, due to the feature of self-generation of carriers by muon implantation. This contrasts with the other probes of spin dynamics, which are more suited to the highly doped metallic state.

Details of the μSR technique have been reviewed elsewhere (e.g. [4]) and some of the earlier muon work on conducting polymers was covered in a previous review [5]. In this paper we review the current status of experimental and theoretical studies of muon-detected carrier motion in conducting polymers. The paper is organized in four parts. The first section reviews the early development of the field, which focused on the prototypical conducting polymer, polyacetylene, and on developing appropriate models to link the observed relaxation with the microscopic diffusion parameters. The second part explores in more detail the most well-developed relaxation model for a bound muon interacting with mobile carriers, the Risch–Kehr model. The third part covers experimental studies on a range of conducting polymers, which generally have non-degenerate bond-alternation ground states, supporting electronic excitations in the form of polarons rather than solitons. The conclusion summarizes the current experimental and theoretical status and highlights some possible directions for future development in this field.

1. Polyacetylene and 1D diffusion models

The first muon relaxation experiments on the conducting polymers were carried out by Nagamine and co-workers in the mid-1980s on the simplest conducting polymer, polyacetylene (PA) [6–11] (see figure 1). Implanted muons were used to probe the properties of mobile spin excitations in the *trans* isomer of PA. In these studies the longitudinal muon spin relaxation was measured and the main source of muon relaxation was attributed to hyperfine coupling between muons bonded to the polymer and mobile electronic excitations in the form of solitons [12], which are able to move relatively freely along the polymer chain. The data were analysed using an exponential relaxation function and an expression was used for the relaxation rate which was originally derived for NMR in an anisotropic system with diffusive spin motion [13, 14]. The longitudinal relaxation rate λ may be written as [13]

$$\lambda(B) = \frac{\rho}{20}[3D^2 f(\omega_\mu) + (5A^2 + 7D^2) f(\omega_\mathrm{e})] \tag{1}$$

where $\omega_\mu = \gamma_\mu B$, $\omega_\mathrm{e} = \gamma_\mathrm{e} B$, ρ is the spin concentration, A and D are the scalar and dipolar hyperfine coupling parameters and $f(\omega)$ is the spectral density of the spin correlation function, which contains the information about the spin dynamics. For a purely one-dimensional (1D) diffusion process, the correlation function for a particle revisiting the origin has a $t^{-1/2}$ behaviour, so the associated spectral density derived by Fourier transformation is $f(\omega) \propto \omega^{-1/2}$, which implies that there should be a $B^{-1/2}$ scaling in the relaxation rate; this was indeed observed in the experiment (figure 2).

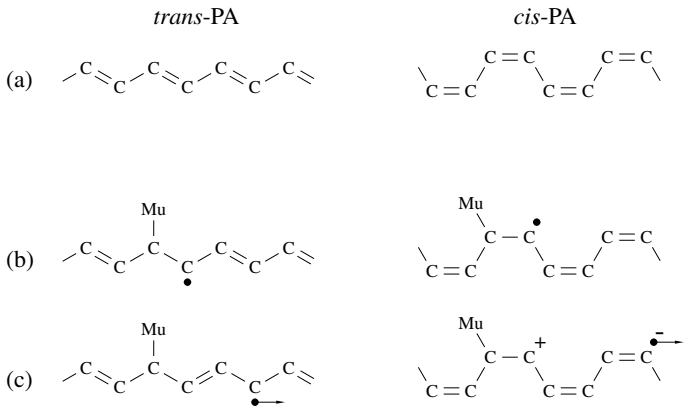

Figure 1. (a) The two isomers of PA and (b) the unpaired electron state formed by addition of muonium to the chain. (c) In the *trans* case, degeneracy of the possible bond-alternation ground states leads to solitonic spin defects in the form of mobile bond-order domain walls [12]. Consequently the muon-generated spin defect can move freely away from the muon site as a neutral soliton, In contrast, the *cis* isomer lacks the degenerate bond-alternation ground state of the *trans* isomer and free solitons are not supported. In this case the spin defect can still move away in the form of a negative polaron, leaving behind a positive charge near the muon site. Note that although the spin is represented here as being localized at one site, the spin structure is actually spread out over 20–30 sites.

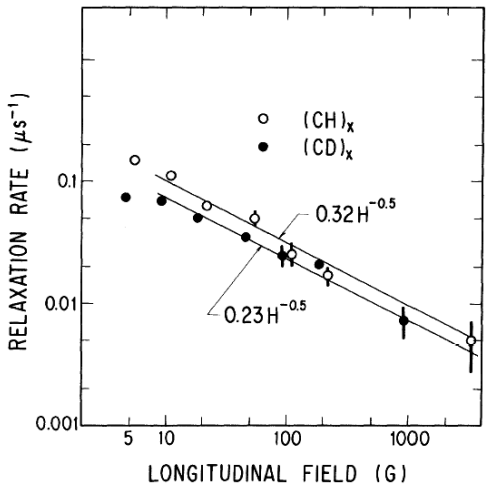

Figure 2. The field dependence of the fitted exponential muon relaxation rate λ for *trans*-PA [7]. The very smallness of the isotope effect and the $H^{-1/2}$ field dependence indicate that the muon spin relaxation is dominated by coupling to mobile electronic spin excitations in the form of solitons.

In the *cis* isomer of PA, a completely different behaviour was seen; very small residual asymmetry was measured at low fields with only very weak relaxation. A clear repolarization effect was observed, where applying small longitudinal fields led to a recovery of asymmetry; full asymmetry was regained for fields above 100 G. This behaviour was attributed to trapping of the soliton at the muon site, due to the absence of degeneracy in the bond-alternation ground state for this isomer. In the trapped state it is possible to make a spectroscopic measurement of the hyperfine coupling between the spin defect and the muon. Values for A in the region

of 91 MHz were obtained for several samples of *cis*-PA using high transverse field muon spin rotation and level-crossing-resonance techniques [9]. When the spin is highly mobile, however, such spectroscopic measurements become impossible, due to the large dynamical broadening effects. In this situation direct relaxation measurements in the time domain become the only viable experimental technique. On the theoretical side, the difference in the structure and properties of the extended spin defect for the two isomers on addition of muonium was calculated by Fisher *et al* [15] and shown to be consistent with the experiments.

The time evolution of the relaxation was observed in the experimental studies to be non-exponential; this was originally interpreted in terms of interchain motion of solitons. However, it is known that the correlation function for 1D diffusion is not an exponential and hence the muon spin relaxation is not expected to be a simple exponential either. Risch and Kehr (RK) [16] furthermore pointed out that since the correlation time for the return to the origin of a particle diffusing in 1D is divergent, the standard NMR theory used for the earlier data analysis is not strictly valid, as it assumes the existence of a finite correlation time that is short compared to all other timescales in the problem. RK then applied a stochastic diffusion theory to the model of a static muon interacting through an intermittent hyperfine coupling with an electron that is randomly diffusing along a 1D chain. They derived the corresponding non-exponential relaxation function and obtained an inverse field dependence for the relaxation parameter Γ. This predicted relaxation behaviour has been found to describe the measurements in conducting polymers rather well [16, 25]. The RK theory will be covered in more detail in section 2.

Although it may be difficult to observe the interchain motion directly in the time domain through its contribution to the muon relaxation function, interchain motion is expected to provide a cut-off to the divergence of the measured relaxation rate as the probe frequency is reduced by lowering the applied magnetic field. This interchain motion can be included in the conventional relaxation rate theory by generalizing the motion to an anisotropic random walk on a discrete lattice. Butler *et al* [14] showed that the correlation function describing the probability of return to the origin for a particle performing a random walk on a discrete lattice, with site-to-site hopping rates D_1, D_2 and D_3 along the three axes of the lattice, is given by the expression

$$\phi(t) = \mathrm{e}^{-2(D_1+D_2+D_3)t} I_0(2D_1t) I_0(2D_2t) I_0(2D_3t) \tag{2}$$

where I_0 is the modified Bessel function. The corresponding spectral density function is derived from the Fourier transform of equation (2). For the quasi-1D case that we are particularly interested in, $D_1 = D_\parallel$ is identified with the fast intrachain diffusion rate and $D_2 = D_3 = D_\perp$, the slower interchain diffusion rate. In the regime where $\omega \ll D_\parallel$, the spectral density function is then given by [17, 18]

$$f(\omega) = \frac{1}{\sqrt{4D_\parallel D_\perp}} \sqrt{\frac{1+\sqrt{1+(\omega/2D_\perp)^2}}{1+(\omega/2D_\perp)^2}}. \tag{3}$$

The effect of the cut-off shown by equation (3) on the frequency dependence of the relaxation rate is illustrated in figure 3. In the case of the RK model, which does not explicitly include interchain processes, an empirical cut-off of the form $\Gamma = \Gamma_0/(1+\omega/D_\perp)$ has been used in analysing experimental data; this can be seen to provide a softer cut-off than equation (3). If a low frequency cut-off can be observed in a measurement, then both $D_\parallel$ and $D_\perp$ can be estimated from the field dependence of the relaxation rate. However, other effects can compete to produce a low field cut-off, as will be seen in the following section, and care must be taken in assigning the cut-off to an interchain diffusion process.

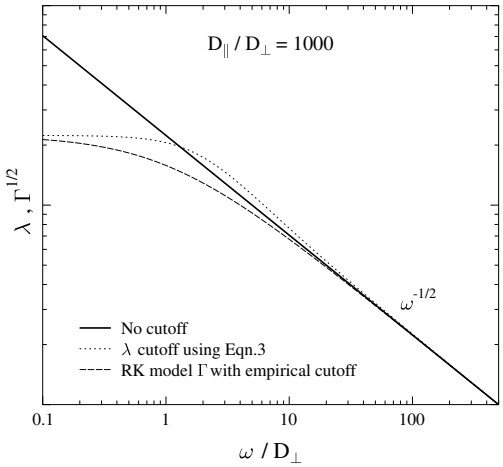

Figure 3. The field dependence of the muon relaxation rate λ or $\Gamma^{1/2}$ for 1D diffusion models, along with the effect of introducing a cut-off reflecting interchain diffusion.

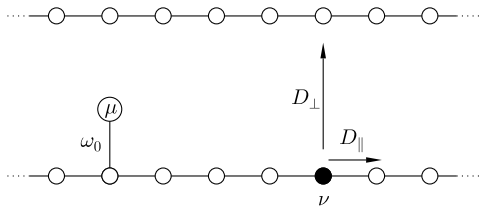

Figure 4. The RK model involves a muon bound to a single site in the chain with an electron hopping freely along the chain with diffusion rate labelled $D_\parallel$ ($=\gamma/2$). The electron interacts with the muon via the hyperfine coupling ω_0, but only when it occupies the site adjacent to the muon. While it diffuses, the electron spin relaxes at the rate ν due to interaction with other spins distributed throughout the system. The interchain hopping rate $D_\perp$ is also included as an extension to the original model.

2. The Risch–Kehr model

Although the RK model appears quite simple, with only three microscopic parameters, the predicted muon relaxation behaviour is remarkably complex and it is useful to explore the predicted behaviour in some detail, in order to help in identifying its experimental signature in comparison with other possible models for the dynamical behaviour. The three parameters in the RK model [16] (see figure 4) are the hyperfine coupling ($\omega_0 = 2\pi A$, assumed isotropic), the electron spin relaxation rate (ν, resulting from interaction with spin defects or excitations of the lattice) and the on-chain site-to-site hopping rate $D_\parallel$. The RK formulae are expressed in terms of the total hop rate parameter γ, which is twice $D_\parallel$ (note that this hop rate γ should not be confused with the gyromagnetic ratios γ_μ and γ_e). The on-chain diffusion constant is related to the diffusion rate by $\mathcal{D}_\parallel = D_\parallel a^2$, where a is the site separation. The muon relaxation function is then determined by these three parameters plus the time dependent probability function for the electron's return to the origin $F(t)$. $F(t)$ contains all the information about the mechanisms and dimensionality of the diffusion and could in principle include such additional factors as interchain hopping, reflection at chain ends and trapping sites or the presence of an initial activation barrier at the muon site. In the systems with highly mobile spin excitations, the magnitude of the three parameters will typically follow the order $\gamma > \omega_0 > \nu$.

RK gave full expressions for the polarization behaviour in the Laplace domain (see equations (40)–(43) in [16]). Although these expressions are rather complex, numerical inversion to give the time evolution of the muon polarization can be performed and we have used the algorithm of D'Amore *et al* [24] to perform this inversion and evaluate the form of the muon spin relaxation function in different situations. Asymptotic expansions were also given by RK for several parameter regimes.

In the rest of this section we survey the main results of the RK model, before looking in section 3 at applications of the muon technique to conducting polymer systems other than PA.

2.1. The fixed electron model

It is useful to make a comparison with the relaxation behaviour expected for a fixed electron in a bound muonium state, before looking in detail at the effects of electron motion on the muon spin relaxation. In this case there is no diffusion of the spin, but the electron is subject to spin relaxation by interaction with an external thermal reservoir. The Wangsness–Bloch dynamical model [19] can be used to calculate the relaxation behaviour and its magnetic field dependence. This involves solving the equation of motion for the density matrix of the hyperfine-coupled muon–electron system. Fifteen coupled equations are obtained, describing the three components of muon polarization, three of electron polarization and the nine mixed polarization components [20–22]. The electron relaxation rate is introduced as a constant term $-\nu$, which is added to those diagonal elements of the dynamical matrix that describe the electron or mixed polarization. In principle, the resulting relaxation function for the muon spin could be quite complex, containing a large number of precessing and exponentially relaxing components, particularly when anisotropy of the hyperfine interaction is taken into account. However, we have found that in practice, for most reasonable parameter values, the non-oscillatory part of the muon relaxation is dominated by a single-exponential decay. In this situation a conventional exponential muon spin relaxation function

$$G_z(t) = \mathrm{e}^{-\lambda t} \tag{4}$$

is expected to be observed and figure 5 shows the corresponding field dependence expected for the relaxation rate λ in this case. Parameter values are taken to be those typical for a paramagnetic muon state in a conjugated polymer. The relaxation rate is described by the expression

$$\lambda = \frac{\nu}{1 + (\frac{\omega_e}{\omega_0})^2} \tag{5}$$

in which the muon closely follows the electronic relaxation at low fields but becomes progressively decoupled at higher fields with a corresponding reduction in the muon spin relaxation rate.

2.2. Field dependence of the relaxation

In the RK model the general form of the muon spin relaxation function, away from the earliest times, takes the form

$$G_z(t) = \mathrm{e}^{\Gamma t}\mathrm{erfc}\sqrt{\Gamma t} \tag{6}$$

where erfc represents the complementary error function. Equation (6) shows $t^{-1/2}$ behaviour at long times, following the behaviour of the 1D correlation function. In terms of the microscopic parameters of the model, the relaxation rate parameter is given by

$$\Gamma = \frac{\nu}{\left(1 + \gamma\frac{\sqrt{2\omega_e\nu}}{\omega_0^2}\right)^2}. \tag{7}$$

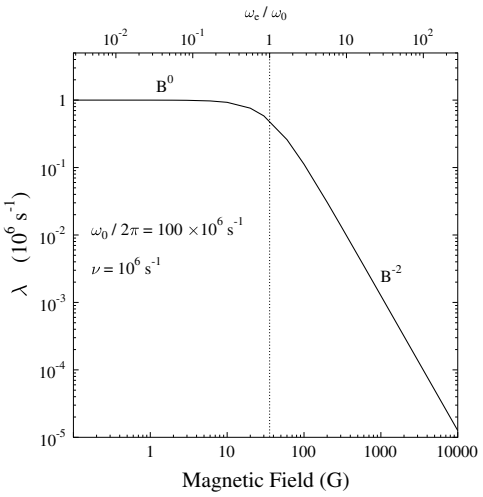

Figure 5. The field dependence of the exponential muon relaxation rate λ for a static electron with spin flip rate $\nu = 10^6\ \mathrm{s}^{-1}$ and hyperfine coupling $A = 100$ MHz.

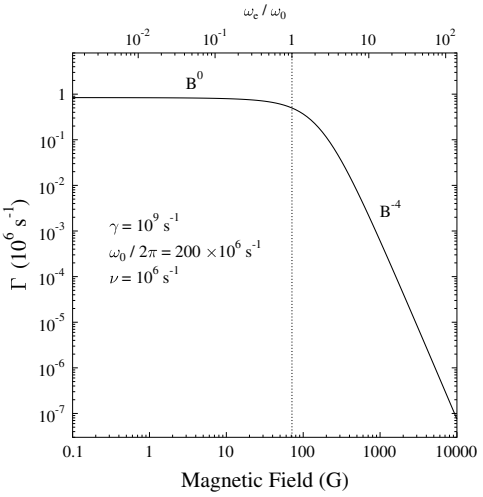

Figure 6. Field dependence of the RK relaxation rate Γ in the quasistatic limit of slow electron diffusion where $\gamma < \omega_0$. A sharp cut-off takes place when ω_e becomes greater than ω_0.

When the field is high enough for the second term in the denominator of equation (7) to dominate, this becomes independent of ν:

$$\Gamma = \frac{\omega_0^4}{2\omega_\mathrm{e}\gamma^2}, \tag{8}$$

exhibiting the characteristic B^{-1} behaviour for Γ.

The purely static regime where $\gamma = 0$ was discussed in section 2.1. If γ is finite but slow compared to ω_0, then the relaxation behaviour can be regarded as quasistatic, with a similar high field cut-off behaviour to the static case (figure 6). In this regime the relaxation rate remains constant up to the cut-off field, at which $\gamma = \omega_\mathrm{e}$, followed by a steep B^{-4} fall-off at high fields. Note that for the low relaxation rates expected at high fields, it may be difficult to distinguish the RK relaxation function of equation (6) from the simple exponential of equation (4) over the timescale of a typical μSR measurement. The behaviour shown in figure 6 is then equivalent to that of figure 5, apart from the factor of two in the power law, due to the different scaling properties of the two relaxation functions when the relaxation rate is small.

When the diffusion rate is significantly larger than the hyperfine frequency, an appreciable regime appears in which Γ follows B^{-1} according to equation (8) (figure 7). If such a regime can be observed, then equation (8) can be used to estimate the diffusion rate from the measured Γ, as was done in previous studies (e.g. [25, 26]). However, some independent knowledge of ω_0 is required to get an accurate measurement of γ. In principle this can be obtained from the decoupling behaviour, but the usual static decoupling theory will not strictly be applicable here and the dynamics needs to be taken fully into account when estimating ω_0 from the repolarization curve. We will return to this point later.

A high field cut-off will also eventually be seen in the fast diffusion case as ω_e approaches and exceeds γ (figure 7); the power law in the high field regime is again B^{-4}. Note that in contrast to the static and quasistatic cases, in this parameter regime there is no particular crossover feature around $\omega_\mathrm{e}/\omega_0 = 1$, which appears here in the middle of the 1D region.

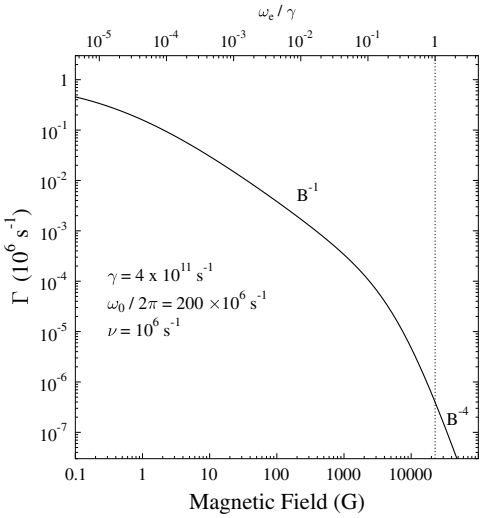

Figure 7. The field dependence of the RK relaxation rate in the fast diffusion limit ($\gamma > \omega_0$), where a broad region of 1D behaviour is apparent. A high field cut-off is seen when $\omega_e > \gamma$ and at high fields Γ follows a B^{-4} law.

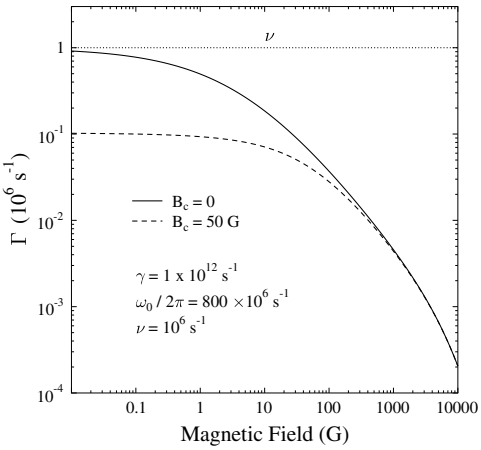

Figure 8. The field dependence of the RK relaxation rate in the fast diffusion limit where 1D inverse field relaxation behaviour is apparent at high fields, with and without an additional low field cut-off at 50 G.

The overall picture that one obtains for the high field cut-off is that it is determined by the probe frequency becoming faster than the fastest characteristic frequency of the system; in the static and quasistatic cases this frequency is the hyperfine frequency ω_0, whereas in the presence of fast diffusion it is the hop rate γ. Above the cut-off field the relaxation rates become significantly reduced and, due to the dominance of the square root in equation (6) at low Γt, the B^{-4} behaviour for the RK relaxation scales closely with the B^{-2} behaviour expected from a standard Lorentzian spectral density function.

It should be noted that while the spin is diffusing, the presence of a finite value of ν, that is significantly smaller than both ω_0 and γ, is essential for the muon to see the characteristic field dependence of the low dimensional motion. This was demonstrated in a computer simulation reported by Jestädt *et al* [23], who studied a 1D diffusion model in which the electron spin polarization is lost completely every time the electron leaves the muon site, regardless of the time elapsed between return visits. This corresponds to the fast electron relaxation limit $\nu > \gamma, \omega_0$. Although the RK relaxation function, equation (6), was clearly observed in the simulation in the time domain, the field dependence of the relaxation rate simply showed a high field cut-off and did not have any extended region with $\Gamma \propto B^{-1}$ or $\lambda \propto B^{-1/2}$.

2.3. The low field cut-off

On the low field side there is an intrinsic cut-off to the B^{-1} behaviour, as reflected in equation (7), once Γ approaches the electron spin relaxation rate ν, as the muon cannot relax faster than the electron in this model. If ν is sufficiently fast, then the low field cut-off may be defined by features of the diffusion topology, as discussed earlier, rather than by ν. Information about the interchain diffusion rate may then be inferred from such a cut-off (figure 8). Note that this implies that for studying transport related cut-off phenomena, ν should be as large as possible, while still being small compared to ω_0^2/γ, in order to observe relatively slow cut-off frequencies related to interchain motion.

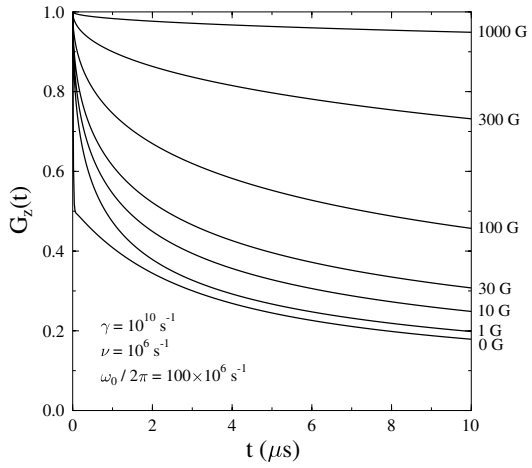

Figure 9. An example showing the field dependence of the muon spin relaxation in the RK model with the parameters shown.

2.4. The low field relaxation function

The low field relaxation can be quite different from the higher field behaviour. In zero field and for slow ν the relaxation takes an exponential form at early times [16], following

$$G_z(t) = (1 + \mathrm{e}^{-{\omega_0}^2 t/\gamma})/2, \tag{9}$$

which shows a polarization plateau at 0.5, reflecting the expected residual polarization for free muonium. Allowing for electron relaxation, the plateau relaxes and on increasing to moderate fields (figure 9) the relaxation takes the form of the RK function at longer times (equation (6)), with the value of Γ given by

$$\Gamma = \frac{\nu}{(1 + (\gamma\nu/\omega_0^2))^2}. \tag{10}$$

If ω_0 is relatively large and γ relatively small, then the initial exponential relaxation may be too fast to measure and will appear as a lost asymmetry fraction, which may be recovered by applying a magnetic field. Numerical calculations are however necessary to adequately describe the transition from this very low field regime to the higher field regime and test its dependence on ω_0 and the other parameters involved. RK gave an exact expression in Laplace space for zero field (RK equations (44), (45)), which can be inverted numerically to demonstrate the dependence of the zero-field relaxation on the diffusion rate (figure 10).

2.5. Repolarization and relaxation

The absolute accuracy of γ estimated from a measurement of Γ depends on accurate knowledge of ω_0, which may be difficult to obtain in practice. In the static case, a reasonable estimate of ω_0 may be determined from the mid-point of the repolarization. In the presence of fast dynamics the determination of ω_0 is not so straightforward. However, by studying together both the repolarization of asymmetry at fixed time and the field dependent relaxation rate, it should be possible to derive values for the two parameters γ and ω_0 self-consistently. If a time is chosen where the relaxation follows the RK function, then the Laplace domain expressions (RK equations (54), (55)) can be inverted and used for fitting the data. The repolarization behaviour expected for different diffusion rates is shown in figure 11 together with the corresponding field dependences for the relaxation rate.

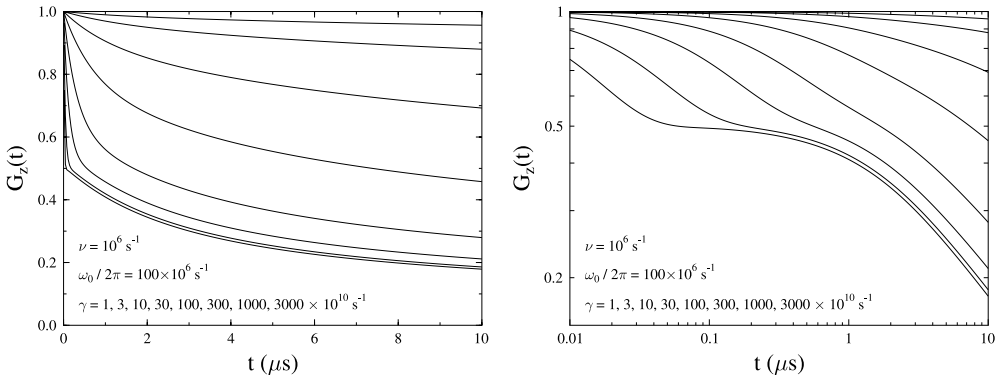

Figure 10. The zero-field muon spin relaxation function as the electron diffusion rate varies, with linear time and log time plots shown for the same numerical data.

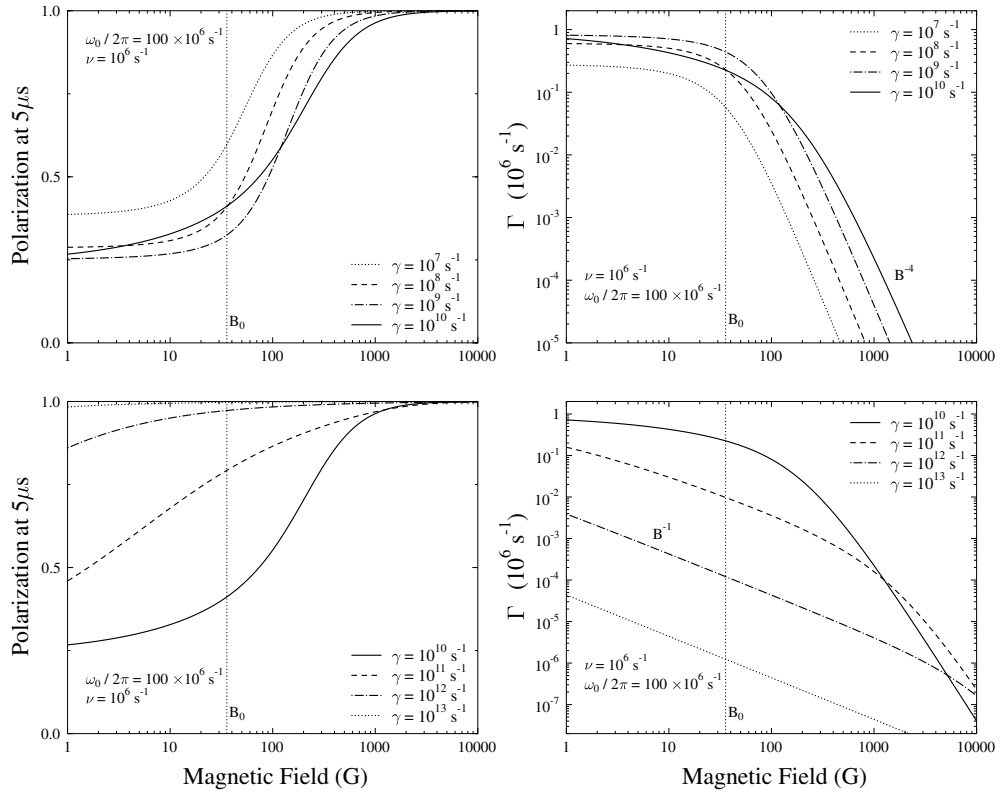

Figure 11. The muon spin repolarization curves (left-hand side) and RK relaxation rate Γ (right-hand side) as the electronic diffusion rate increases with fixed ν and ω_0. B_0 is the mid-point of the static repolarization determined by ω_0.

For the lowest values of γ shown, the repolarization is quite similar to the standard static case. Moderate 1D diffusion rates shift the centre of the repolarization (defined as the 75% polarization point) to higher fields and broaden the repolarization compared to the static case. At higher diffusion rates the broadening becomes more extreme and the centre of the

repolarization feature goes through a maximum and then moves rapidly to lower fields and disappears completely, as the muon and electron become strongly decoupled at the fastest diffusion rates and the polarization remains high at all fields. The presence of a broad repolarization curve combined with an extended region where $\Gamma \propto B^{-1}$ may be taken as a characteristic feature of this type of coupled muon–electron dynamics which is governed by fast 1D diffusion of the electron.

3. Application to various conducting polymers

Since *trans*-PA is rather unique in having a degenerate bond-alternation ground state that supports free neutral solitons, it was not initially clear whether the muon technique would be of use in the more usual non-degenerate systems, where bond-alternation solitons are not free to move. Indeed, as discussed in section 1, the data for the non-degenerate *cis* form of PA showed a bound spin defect associated with the muon, with very little relaxation. In the majority of conducting polymers, which cannot support free solitons because of their non-degenerate ground states, the simplest mobile carriers are charged polarons. These polarons should also move according to the anisotropic diffusion models that have been considered earlier. In the case of a muon-generated carrier, a negative polaron is formed, which will leave a positive charge if it diffuses away from the muon site (figure 1). Hence there is an energy of binding to the muon site which may lead to localization of the polaron. The site of muonium addition could be regarded as a semiconductor donor state requiring ionization to produce a mobile polaronic charge carrier. In general, conducting polymers are found experimentally to have a muon spin relaxation behaviour that has features in common with both *trans*-PA and *cis*-PA, i.e. a significant field dependent relaxation is seen together with a repolarizing component of asymmetry. This suggests the presence of both localized and mobile spins within the same sample. If this is the case then the tendency to localization near the muon must be dependent on the local environment. Various factors may determine the degree of localization. The extended nature of the wavefunction of the polaron and the high polarizability of the conjugated electron system would both tend to reduce the electrostatic binding potential. There will also be changes in the local electronic structure when the muon is bonded to the chain. All these factors would need to be taken into account to determine whether the polaron is bound in a particular configuration in a specific system. Even in the case where the muon-generated polaron is strongly bound to the muon site, it can provide a sensitive probe for the motion of the small concentration of other polarons generally present in these organic semiconductors (further polarons may also be generated by radiolytic processes associated with the muon implantation). These polarons may be free to move and interact with the bound polaron and its closely coupled muon via a spin exchange mechanism.

Another possibility to consider is whether the muonium is completely thermalized when it reacts with the chain; any excess energy brought into the reaction could be carried away by a polaron, which would only become trapped once it had completely thermalized and diffused back to the muon site. Since this return process would be governed by anisotropic diffusion, one might expect in this case to see a characteristic field dependence very similar to that of the continuous diffusion model. Other types of 'hot' process including bond rupture may also be possible during the implantation stage as the muon slows down towards its final state. These processes are mostly expected to take place a considerable distance away from the bonding site of the muonium. In determining the significance of such processes for the muon studies one should consider the muon spin relaxation associated with such states. The situation where such a process might have the greatest effect on the observed muon spin relaxation is where the muonium energy at the end of its track is just enough to break the chain and simultaneously

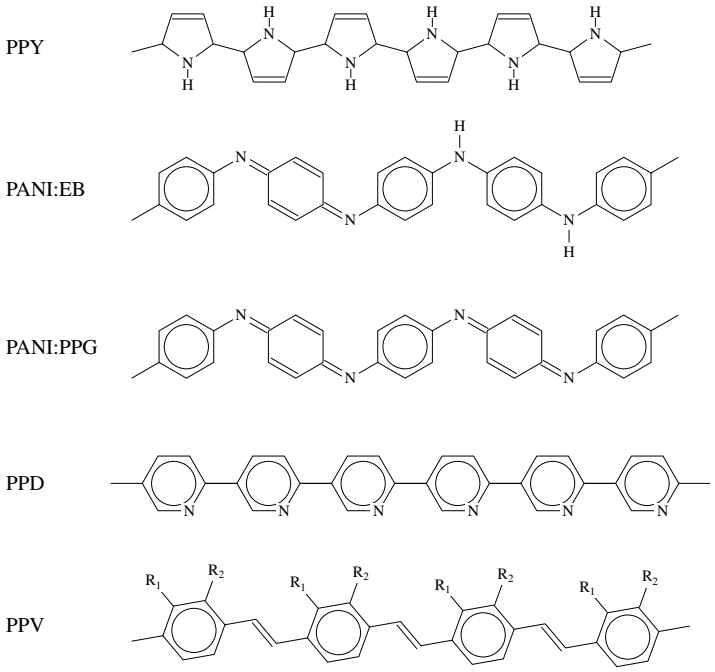

Figure 12. The structures of the polymers, in addition to polyacetylene, for which muon studies have been reported. From top to bottom these are polypyrrole (PPY), polyaniline:emeraldine base (PANI:EB), polyaniline:pernigraniline base (PPG), polypyridine (PPD) and polyphenylenevinylene (PPV).

bond to one side of the rupture. The unpaired spin in this case would however be on the opposite segment to that containing the muon and the hyperfine coupling would be very weak compared to the standard picture of a polaron produced on the same chain as the muon.

In the rest of this section we will review the experimental results that have been obtained for various conducting polymers using muons. Molecular structures for these polymers are shown in figure 12.

3.1. Polypyrrole

Polypyrrole (PPY) was the second conducting polymer system to be studied by means of muons, following the original pioneering work on PA by the Tokyo group. In undoped PPY, the polarons were observed to be strongly localized at 15 K, showing similar behaviour to that seen in *cis*-PA, with very little relaxation [27]. At 300 K, however, a much stronger relaxation appeared and the field dependence of the relaxation rate was found to be well fitted by a two-dimensional (2D) diffusion model for the polarons.

Studies of PPY doped into the metallic state were also made [28, 27, 30]. In the doped polymers full diamagnetic asymmetry was seen. As in normal metals, paramagnetic muon states are not stable here. The electronic contribution to the relaxation was found to be much weaker compared to the undoped case. This reflects the lack of the large contact hyperfine coupling that would be associated with a chemically bonded muon state. Consequently the electronic relaxation competes with relaxation due to dipolar fields from nuclear spins. The lack of a chemical bond between the muon and the polymer also allows the muon to diffuse

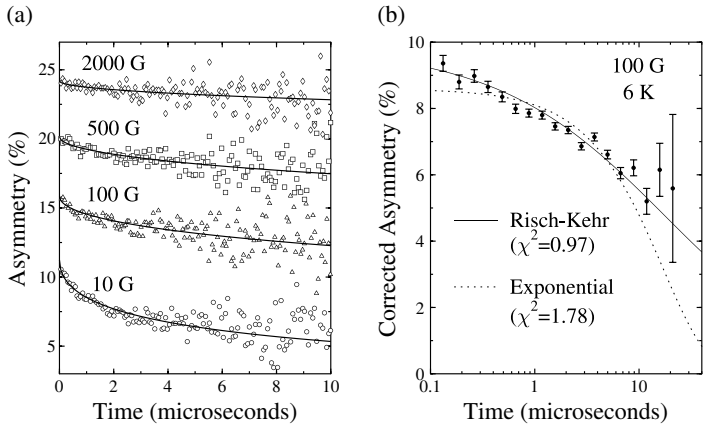

Figure 13. (a) Muon spin relaxation in PANI:EB at 6 K; the solid curves are RK relaxation fits. (b) Comparison of RK and exponential relaxation fits [25].

at high temperatures, which further complicates the data analysis. Provided that the electron motion is faster than the muon motion, however, information about the electronic diffusion may still be obtained. The temperature dependence of the electronic relaxation rate in toluene sulfonate-doped PPY indicated that the carrier diffusion rate decreases significantly with decreasing temperature [28], consistent with the changes observed in macroscopic conductivity measurements. Differences in the low temperature spin dynamics were seen between materials doped with PF_6 and with toluene sulfonate ions [30], which were also found to be correlated with macroscopic transport measurements.

3.2. Polyaniline

Two non-metallic forms of polyaniline (PANI), emeraldine base (EB) and polypernigraniline base (PPG) were studied and found to show $B^{-1/2}$ behaviour in the relaxation rates derived from fitting to exponential relaxation functions at low temperatures; this is consistent with 1D carrier motion [27]. PPG is of particular interest, as it is one other example, besides *trans*-PA, of a system with a degenerate ground state which can support free solitons. In the case of PANI:EB an interchain cut-off could be observed in the field dependence at higher temperatures. In subsequent studies the RK relaxation function (equation (6)) was shown to provide a better fit of the relaxation data (see figure 13). The relaxation rate Γ was observed to show B^{-1} scaling over a wide range of fields (figure 14) and using the RK model with low field cut-off, with ω_0 being estimated from the repolarizing asymmetry (figure 13), the intrachain and interchain diffusion rates could be extracted over a range of temperatures (figure 15) [25, 31]. The temperature dependence of the interchain diffusion rate was found to be similar to that seen in ESR studies of doped material [18], indicating relatively slow thermally activated transport. In contrast, the fast intrachain motion was found to be less temperature dependent, showing a phonon-limited dependence, characteristic of metal-like transport. Interaction of the polarons with thermally activated ring libration modes was found to give a good description of the temperature dependent data (figure 15).

The metallic state of polyaniline, emeraldine salt (PANI:ES), has also been studied [32, 29, 30]. The electronic contribution to the relaxation was found to be best described by a 2D diffusion model, as was found to be the case for doped polypyrrole. The measured

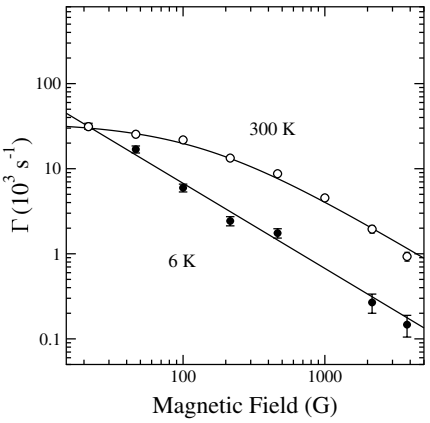

Figure 14. Comparison between the field dependence of Γ observed in PANI:EB at 6 K and at 300 K [25].

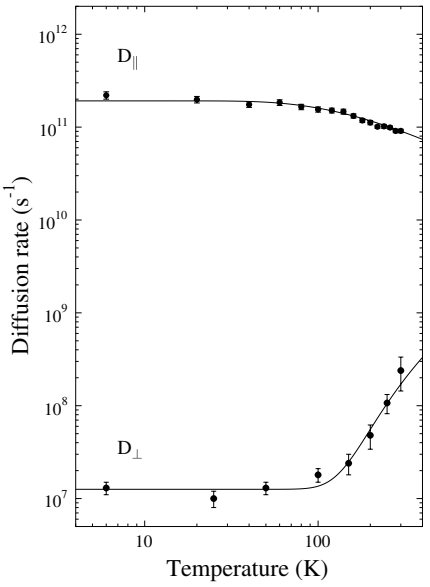

Figure 15. The temperature dependence of the intrachain $D_{\|}$ and interchain $D_{\perp}$ diffusion rates in PANI:EB [25, 31].

temperature dependence implied that intrachain diffusion rate increases with temperature in the metallic state, in contrast to the undoped case, but in agreement with the results from ESR studies of PANI:ES [18]. This presumably reflects the tendency to localization at low temperatures produced by the dopant ion potential, which is not present in the undoped case.

3.3. Polypyridine

Polypyridine (PPD) is a conducting polymer which is particularly efficient at transporting negatively charged carriers and hence is useful for organic light-emitting-diode applications [33]. Muon spin relaxation studies have been used to study the motion of negative polarons in PPD [31]. The low temperature intrachain diffusion rate was found to be similar to that of PANI:EB (see figure 16), being independent of temperature below 100 K. The diffusion rate maintains a high value over a wide range of temperature and then falls off above 200 K. This can be compared with the PANI case where the onset of the fall is around 50 K. The high temperature behaviour here is controlled by scattering from a lattice mode with an energy

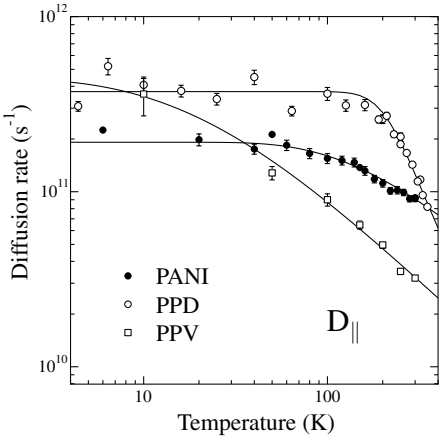

Figure 16. Comparison between temperature dependent diffusion rates for three different conducting polymers determined by μSR [34].

around 90 meV, compared to a 12 meV mode in the PANI case. This difference reflects the rather different structures of the two polymers (see figure 12); whereas the rings in PANI are free to rotate about flexible links through the nitrogens, the structure of PPD is much more rigid, with direct linkage of the rings through single bonds. The rings can therefore maintain good alignment over a greater range of temperature, which is beneficial for the transport properties.

3.4. Polyphenylenevinylene

Polyphenylenevinylene (PPV) is a polymer system that has been found to be well suited to the fabrication of electroluminescent display devices and understanding the physics of carrier motion in these materials is of great technological interest. The properties of PPV can by tailored by adding long side chains to increase chain separation and improve the fluorescence and electroluminescence quantum yields. This would also be expected to modify the microscopic carrier diffusion rates and the muon spin relaxation technique has recently been applied to study these effects [26]. Polaron diffusion properties were measured for PPVs with two different types of side chain (figure 17). As one might expect, the effect on the intrachain motion of modifying the side chain is not so great. On the other hand, the interchain motion was found to be drastically modified at low temperature (figure 18) with the temperature dependence being described over the range of measurement by a simple thermal activation law where the activation energy differs by a factor of six between the two polymers.

3.5. Biopolymers

Biopolymers are not usually regarded as conducting polymer systems. However, long range motion of charge along the polymeric chain has been indicated by various optical experiments on proteins [36] and on DNA [37]. This is an interesting, although still somewhat controversial area, where muon studies can potentially make a contribution. Recent muon studies on the electron transferring protein cytochrome-c [38] and on DNA [39] have explored the possibility of applying to biopolymers the anisotropic carrier diffusion theory that was developed for the conducting polymers. Using this approach, diffusion parameters can be extracted and studied as a function of temperature. The biopolymers are however considerably more complex structurally than the conducting polymers and interpreting the parameters in terms of microscopic dynamical processes is a challenging task. Some parallel theoretical work can therefore be particularly helpful here. In the case of proteins, computational studies of

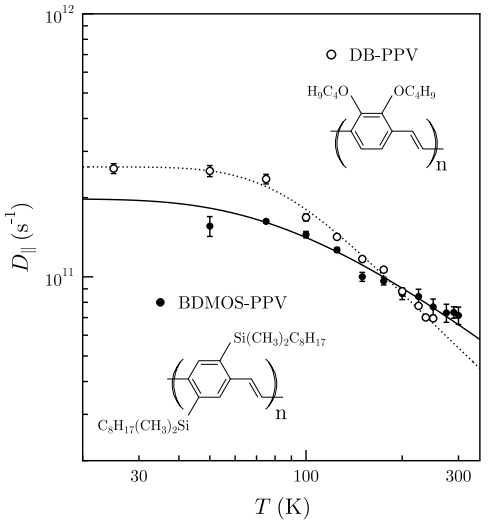

Figure 17. Comparison between the temperature dependent intrachain diffusion rates for two different PPV polymers [35].

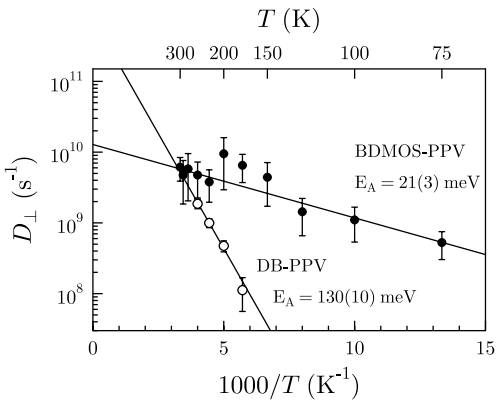

Figure 18. Comparison between the temperature dependent interchain diffusion rates for two different PPV polymers [35].

the muon states in some of the constituent amino acids have been reported [40]. For DNA a theoretical study of muonium adducts of the isolated nucleic acid bases was reported [41], which corresponds well to experiments on these molecules [42]. Such studies are expected to provide useful information for interpreting muon investigations on the full DNA molecule.

4. Conclusion

From the work summarized here it is clear that muons can see evidence for mobile spins in a wide variety of conducting polymers. The initial expectation, that the highly localized muon-generated spins seen in *cis*-PA would be a general characteristic of non-degenerate conjugated polymers, turned out not to be the case. One reason for this may be that *cis*-PA is particularly susceptible to structural distortion when the muonium is added, e.g. a local isomerization to *trans*-PA around the muon site might occur, leading to strong localization of the spin. In contrast, in the case of polymers containing rings, the structures will have an extra stability provided by the ring geometry and such an extreme conformational change would not be possible.

The muon studies complement well the other spin dynamical probe techniques, being particularly well suited to studies of the undoped state. There is also a contrast between the

negative polarons generated by the muon and the positive polarons usually produced by doping and studied by the NMR and ESR methods. Knowledge of the properties of both polarities of polaron is important for polymer device physics, e.g. in electroluminescent devices the balanced injection and recombination of both signs of carrier is required.

Studies of the temperature dependent diffusion rates have revealed the intimate relation between the structural dynamics of the polymer and the motion of the carriers. This reflects the very strong electron–lattice coupling that is a feature of conjugated polymers. Although the temperature dependence of the on-chain diffusion rate can be studied easily with the muon technique, the absolute accuracy of the determination of the on-chain diffusion rate depends on accurate knowledge of the hyperfine coupling, which is not easy to obtain in a highly dynamical regime. We have suggested how an approach combining measurement of both the relaxation rate and the repolarization at a fixed time may be able to simultaneously extract the interdependent hyperfine coupling and diffusion rate parameters.

Another muon technique that can be applied to conducting polymers involves applying electric fields alongside the muon implantation. This technique has found application in muon studies of semiconductors (e.g. [43]). The emerging results on electric field effects in conducting polymers suggest that this technique may be useful in obtaining further information about the muon probe states and the carrier transport mechanisms [44].

While experimental data have been accumulating steadily, there are still many gaps on the theory side. For example, very little has been done to evaluate the changes in local electronic structure produced by the addition of the muon. The interpretation of the observed repolarizing asymmetry as being due to a fraction of localized states is also not entirely certain; attempts to observe these localized spin states spectroscopically have not been successful. The RK model contains a fast relaxation component that is rapidly decoupled by field to produce a repolarization effect extending to early times, so it may be that the experimentally observed repolarization is actually an intrinsic feature of the relaxation function, rather than the result of heterogeneity in the sample. While the RK model has turned out to provide a good basic framework for interpreting the experimental data, it does not include various effects that are expected to occur in real systems, such as interchain hopping, finite chain length and the presence of trap sites. Since the exact analytical solution of the basic intermittent hyperfine coupling model of RK produces a somewhat unwieldy expression in the Laplace domain, further work using numerical simulation in the time domain may be a better way to understand the effect of incorporating these various extensions to the model.

Acknowledgments

The author is grateful for the contributions of many co-workers to the muon studies of conducting polymers, particularly those from his close collaborators W Hayes, K Nagamine and S J Blundell and for the helpful discussions and encouragement of his ISIS colleague S F J Cox.

References

[1] Heeger A J 2001 *Rev. Mod. Phys.* **73** 681
[2] MacDiarmid A G 2001 *Rev. Mod. Phys.* **73** 701
[3] Mizoguchi K 1995 *Japan. J. Appl. Phys.* **34** 19
[4] Blundell S J 1999 *Contemp. Phys.* **40** 175
[5] Hayes W 1995 *Phil. Trans. R. Soc.* A **350** 249
[6] Nagamine K, Ishida K, Matsuzaki T, Nishiyama K, Kuno Y, Morozumi Y, Suzuki T and Yamazaki T 1984 *Hyperfine Interact.* **17–19** 503

[7] Nagamine K, Ishida K, Matsuzaki T, Nishiyama K, Kuno Y, Yamazaki T and Shirakawa H 1984 *Phys. Rev. Lett.* **53** 1763
[8] Ishida K, Nagamine K, Matsuzaki T, Kuno Y, Yamazaki T, Torikai E, Shirakawa H and Brewer J H 1985 *Phys. Rev. Lett.* **55** 2009
[9] Nishiyama K, Ishida K, Nagamine K, Matsuzaki T, Kuno Y, Shirakawa H, Kiefl R and Brewer J H 1986 *Hyperfine Interact.* **32** 551
[10] Nagamine K and Ishida K 1986 *Hyperfine Interact.* **32** 535
[11] Ishida K, Nagamine K and Shirakawa H 1987 *Synth. Met.* **17** 429
[12] Heeger A J, Kivelson S, Schrieffer J R and Su W-P 1988 *Rev. Mod. Phys.* **60** 781
[13] Devreux F, Boucher J-P and Nechtschein M 1974 *J. Physique* **35** 19
[14] Butler M A, Walker L R and Soos Z G 1976 *J. Chem. Phys.* **64** 3592
[15] Fisher A J, Hayes W and Pratt F L 1991 *J. Phys.: Condens. Matter* **3** 9823
[16] Risch R and Kehr K W 1992 *Phys. Rev.* B **46** 5246
[17] Mizoguchi K 1990 *Makromol. Chem. Makromol. Symp.* **37** 53
[18] Mizoguchi K and Kume K 1993 *Solid State Commun.* **89** 971
[19] Wangsness R K and Bloch F 1953 *Phys. Rev.* **89** 728
[20] Nosov V G and Yakovleva I V 1963 *Sov. Phys.—JETP* **16** 1236
[21] Ivanter I G and Smilga V P 1968 *Sov. Phys.—JETP* **27** 301
[22] Meier P F 1982 *Phys. Rev.* A **25** 1287
[23] Jestädt T, Sivia D S and Cox S F J 1997 *Hyperfine Interact.* **106** 45
[24] D'Amore L, Laccetti G and Murli A 1999 *ACM Trans. Math. Softw.* **25** 279
[25] Pratt F L, Blundell S J, Hayes W, Nagamine K, Ishida K and Monkman A P 1997 *Phys. Rev. Lett.* **79** 2855
[26] Blundell S J, Pratt F L, Marshall I M, Steer C A, Hayes W, Husmann A, Fischmeister C, Martin R E and Holmes A B 2002 *J. Phys.: Condens. Matter* **14** 9987
[27] Pratt F L, Hayes W, Mitchell G R, Rossi B, Kiani M S, Malhotra B D, Pandey S S, Milton A and Monkman A P 1993 *Synth. Met.* **55** 677
[28] Pratt F L, Mitchell G R, Cox S F J, Scott C A and Hayes W 1990 *Hyperfine Interact.* **65** 847
[29] Pratt F L, Ishida K, Nagamine K, Pattenden P A, Jestädt Th, Chow K H, Blundell S J, Hayes W and Monkman A P 1997 *Synth. Met.* **84** 943
[30] Pratt F L, Blundell S J, Pattenden P A, Hayes W, Chow K H, Monkman A P, Ishiguro T, Ishida K and Nagamine K 1997 *Hyperfine Interact.* **106** 33
[31] Pratt F L, Blundell S J, Lovett B W, Nagamine K, Ishida K, Hayes W, Jestädt Th and Monkman A P 1999 *Synth. Met.* **101** 323
[32] Pratt F L, Valladares R M, Pattenden P A, Blundell S J, Hayes W, Monkman A P and Nagamine K 1995 *Synth. Met.* **69** 231
[33] Dailey S, Halim M, Rebourt E, Horsburgh L E, Samuel I D W and Monkman A P 1998 *J. Phys.: Condens. Matter* **10** 5171
[34] Pratt F L, Blundell S J, Jestädt Th, Lovett B W, Husmann A, Marshall I M, Hayes W, Monkman A, Watanabe I, Nagamine K, Martin R E and Holmes A B 2000 *Physica* B **289/290** 625
[35] Pratt F L, Blundell S J, Marshall I M, Lancaster T, Husmann A, Steer C, Hayes W, Fischmeister C, Martin R E and Holmes A B 2003 *Physica* B **326** 34
[36] Beratan D N, Onuchic J N, Winkler J R and Gray H B 1992 *Science* **258** 1740
[37] Kelley S O and Barton J K 1999 *Science* **283** 375
[38] Nagamine K, Pratt F L, Ohira S, Watanabe I, Ishida K, Nakamura S N and Matsuzaki T 2000 *Physica* B **289/290** 631
[39] Torikai E, Nagamine K, Pratt F L, Watanabe I, Ikedo Y, Urabe H and Grimm H 2001 *Hyperfine Interact.* **138** 509
[40] Scheibler R H, Cammarere D, Sahoo N, Briere T M, Pratt F L, Nagamine K and Das T P 2003 *Physica* B **326** 30
[41] Oganesyan V S, Hubbard P L, Butt J N and Jayasooriya U A 2003 *Physica* B **326** 25
[42] Hubbard P L, Oganesyan V S, Sulaimnov N, Butt J N and Jayasooriya U A 2004 *J. Phys. Chem.* at press
[43] Storchak V G, Eshchenko D G, Lichti R L and Brewer J H 2003 *Phys. Rev.* B **67** 121201
[44] Pratt F L *et al* 2004 unpublished